Biochimica et Biophysica Acta 1853 (2015) 2885–2896

Contents lists available at ScienceDirect

Biochimica et Biophysica Acta

journal homepage: www.elsevier.com/locate/bbamcr

Modulatory role of the anti-apoptotic protein kinase CK2 in the sub-cellular localization of Fas associated death domain protein (FADD)

Valérie Vilmont [a,b,1], Odile Filhol [c], Anne-Marie Hesse [d], Yohann Couté [d], Christophe Hue [a,e], Léa Rémy-Tourneur [b], Sylvie Mistou [b], Claude Cochet [c,*,2], Gilles Chiocchia [a,e,**,2]

[a] Inserm U1173, Université Versailles-Saint-Quentin, Saint-Quentin-En-Yvelines, France
[b] Inserm U1016, CNRS, UMR 8104, Institut Cochin, Université Paris Descartes, Paris, France
[c] Inserm U1036, Biologie du Cancer et de l'Infection, CEA, Grenoble, France
[d] CEA, DSV, Laboratoire d'Etude de la Dynamique des Protéomes, Grenoble, France
[e] UFR des Sciences de la Santé, Simone Veil, 78180 Montigny-Le-Bretonneux, France

ARTICLE INFO

Article history:
Received 3 July 2015
Received in revised form 28 July 2015
Accepted 1 August 2015
Available online 5 August 2015

Keywords:
FADD
Regulation
Phosphorylation
CK2
Nuclear localization

ABSTRACT

The Fas associated death domain protein (FADD) is the key adaptor molecule of the apoptotic signal triggered by death receptors of the TNF-R1 superfamily. Besides its crucial role in the apoptotic machinery, FADD has proved to be important in many biological processes like tumorigenesis, embryonic development or cell cycle progression. In a process to decipher the regulatory mechanisms underlying FADD regulation, we identified the anti-apoptotic kinase, CK2, as a new partner and regulator of FADD sub-cellular localization. The blockade of CK2 activity induced FADD re-localization within the cell. Moreover, cytoplasmic FADD was increased when CK2β was knocked down. In vitro kinase and pull down assays confirmed that FADD could be phosphorylated by the CK2 holoenzyme. We found that phosphorylation is weak with CK2α alone and optimal in the presence of stoichiometric amounts of CK2α catalytic and CK2β regulatory subunit, showing that FADD phosphorylation is undertaken by the CK2 holoenzyme in a CK2β-driven fashion. We found that CK2 can phosphorylate FADD on the serine 200 and that this phosphorylation is important for nuclear localization of FADD. Altogether, our results show for the first time that multifaceted kinase, CK2, phosphorylates FADD and is involved in its sub-cellular localization. This work uncovered an important role of CK2 in stable FADD nuclear localization.

1. Introduction

Since its discovery in 1995 by Chinnayian et al. as an adaptor of the Fas signaling pathway, the Fas associated death domain protein (FADD) has been described as the main transducer of death domain-containing receptors like TNF-R1 (tumor necrosis factor receptor 1), DR3 (death receptor 3), TRAIL-R1 (TNF-related apoptosis-inducing ligand, DR4), and TRAIL-R2 (DR5) [1–5]. Upon activation of the receptors by their respective ligands, cytoplasmic FADD binds to the intracytoplasmic tail of these receptors via its death domain (DD) and transduces the signal to caspase-8 via homotypic binding of their respective death effector domain. As a result, downstream effector caspases are activated and lead to subsequent cell death [6]. Besides its major role in apoptosis, FADD has been described as a crucial element in many important biological processes like embryonic development, proliferation, cell cycle progression, tumor development, innate immunity and autophagy [7–13]. All these functions are finely tuned via different modes of regulation like phosphorylation and differential localizations [14–16]. While a cytosolic localization is necessary for the pro-apoptotic function of FADD, the role of FADD in cell cycle progression, T cell proliferation or genome surveillance, is dependent on its nuclear localization [17,18]. The exact mechanism of how FADD could participate in anti-apoptoptic processes is still unclear but evidence have shown that phosphorylation of FADD on the residue serine 194 is necessary for the localization of the protein to the nucleus. The CK1α kinase has been identified as the one responsible for FADD phosphorylation and it was shown that CK1α and phosphorylated FADD co-localize in the nucleus during mitosis. The authors suggested that the association with CK1α rather than the phosphorylation itself determined FADD sub-cellular localization [19]. Though it is known that CK1α controls FADD phosphorylation and relocalization to the nuclear

Abbreviations: FADD, Fas associated death domain; CK2, Casein kinase 2; TBB, 4,5,6,7-Tetrabromo-2-azabenzimidazole, 4,5,6,7-Tetrabromobenzotriazole

* Correspondence to: C. Cochet, Inserm U1036, Biologie du Cancer et de l'Infection, iRTSV, CEA, 17 Rue des Martyrs, 38054 Grenoble Cedex 9, France.
** Correspondence to: G. Chiocchia, Inserm U1173, UFR des Sciences de la Santé, Simone Veil, 2 Avenue de la source de la Bièvre, 78180 Montigny-Le-Bretonneux, France.
E-mail addresses: claude.cochet@cea.fr (C. Cochet), gilles.chiocchia@inserm.fr (G. Chiocchia).
[1] Present Address: UMRS 974, Myology Research Center, 105, Boulevard de l'Hôpital, Université Pierre et Marie Curie, Paris, France.
[2] These authors share senior authorship.

http://dx.doi.org/10.1016/j.bbamcr.2015.08.001
0167-4889/

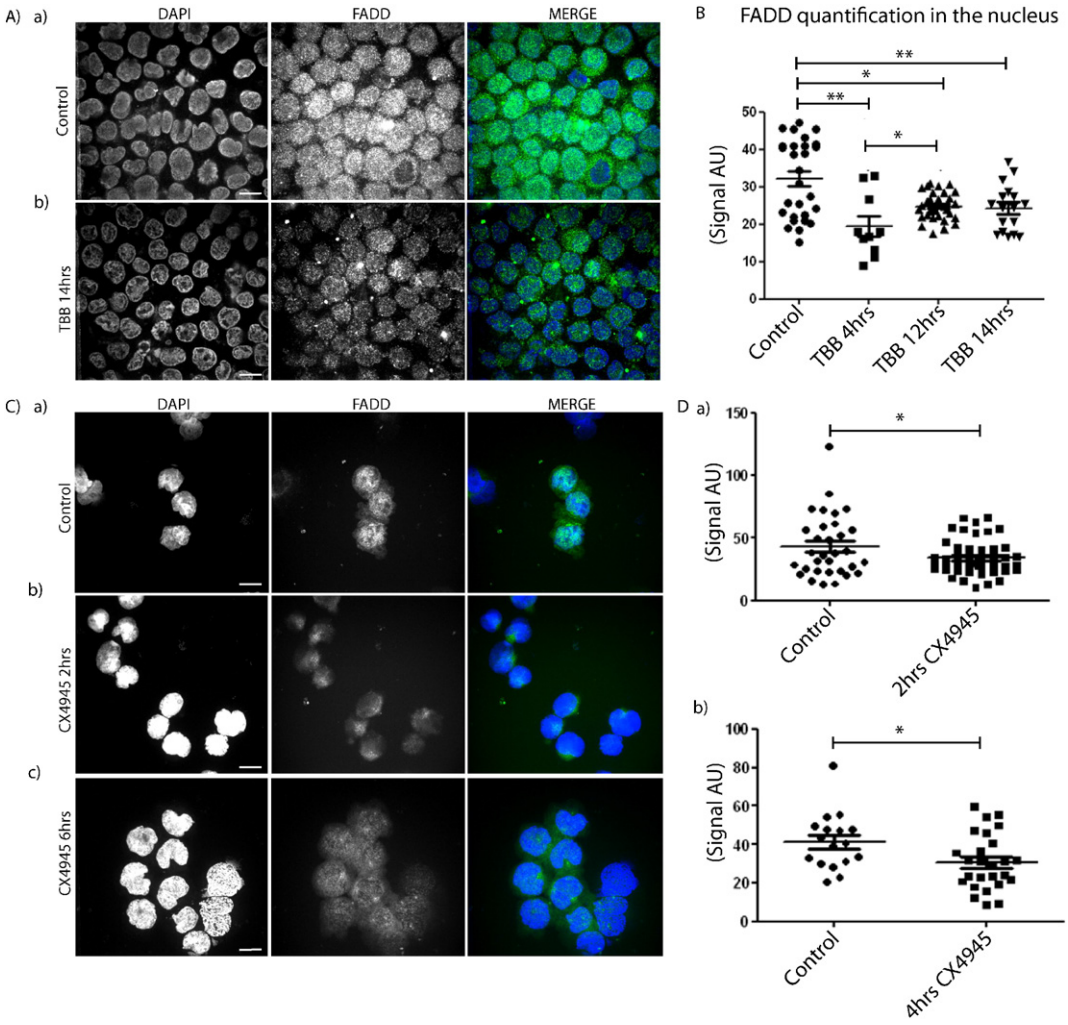

Fig. 1. Imaging of FADD sub-cellular localization upon TBB treatment. THP-1 cells were stained with anti-FADD pAb coupled (green) and DAPI (blue). The cells were incubated in the presence of 50 μM TBB and at different time points. The cells were washed with PBS, deposited on slides using cytospin, fixed and labeled with the indicated antibodies. A) Panel a) is the representative image of untreated THP-1 cells and b) is the representative image of THP-1 cells treated for 14 h with TBB. Data shown are representative of 2 independent experiments and represent the appearance of the majority of cells under a stated condition. Bars represent 10 μm. B) Quantification of nuclear FADD was assessed for each conditions (treated or untreated) using the mask option of Image J. C) Representative image of comparison of FADD localization in (a) untreated cells and cells treated with CX-4945 (20 μg/ml) for (b) 2 h and (c) 6 h. D) Quantification of nuclear FADD assessed using the mask option of Image J. Several image sections were analyzed so that at least 40–50 exploitable cells could be used for quantification. Bars represent 15 μm.*$p \le 0.05$, **$p \le 0.01$ ($n = 2$). **E)** Subcellular fractionation of THP-1 cells. Actin and p84 were used as loading control for cytoplasmic and nuclear extracts respectively. Graphs show quantification of cytoplasmic and nuclear FADD as ratios of FADD signal over actin and p84 respectively. Error bars show SEM of two independent experiments.

compartment, nothing is known about the regulatory means of FADD restriction to the nucleus. This restriction could allow FADD enough time to bind to proteins involved in the anti-apoptotic activities, named above. While searching for such potential regulatory partners of FADD, we focused our attention on the anti-apoptotic protein kinase CK2 [20].

CK2 kinase, formerly casein kinase II, is a highly conserved serine/threonine protein kinase identified in all eukaryotes [20,21]. The protein comprises two alpha catalytic subunits α or α′ and two regulatory subunits β that can form an heterotetrameric holoenzyme in which the two β subunits dimerize to bind to the α or α′ subunits [22,23]. A variety of studies have showed that CK2 is involved in many different cellular processes like cell cycle progression, apoptosis, transcriptional regulation, protein transport, signal transduction and viral physiopathology [20,24–26]. CK2 localizes both in the nuclear and cytoplasmic compartments where it interacts with a wide repertoire of substrates involved in different cellular functions. Of interest, CK2 has been implicated in apoptosis inhibition, cell transformation and also protein localization [27–29]. With regard to functional inhibition of apoptosis, male mice in which the CK2α′ subunit has been disrupted demonstrated a higher number of apoptotic cells in testes than their littermates [30]. In the same line, other studies have shown that CK2 could confer resistance to TRAIL-induced apoptosis in a human model of colon carcinoma cells and FAS sensitivity in a model of endometrial cancer cells by upregulating the level of FLIP, a dominant negative of caspase-8 [27,31]. Studies also showed that CK2 could inhibit apoptosis by blocking caspase cleavage. McDonnell et al. [45] showed in the murine cell line, FL5.12, that CK2 inhibited apoptosis by phosphorylating procaspase-9 near the site of caspase-8 cleavage while Desagher et al., showed that Bid could be phosphorylated by CK2 close to the recognition site of caspase-8 [32]. Consistent with such anti-apoptotic activities, CK2 expression level is therefore increased in several cancers as well as experimental tumors [33]. More specifically, nuclear localization of CK2α was shown to be of poor prognosis in prostate cancer [34]. In light of the anti-apoptotic activities of CK2, we investigated whether a potential regulation of FADD via the kinase could occur.

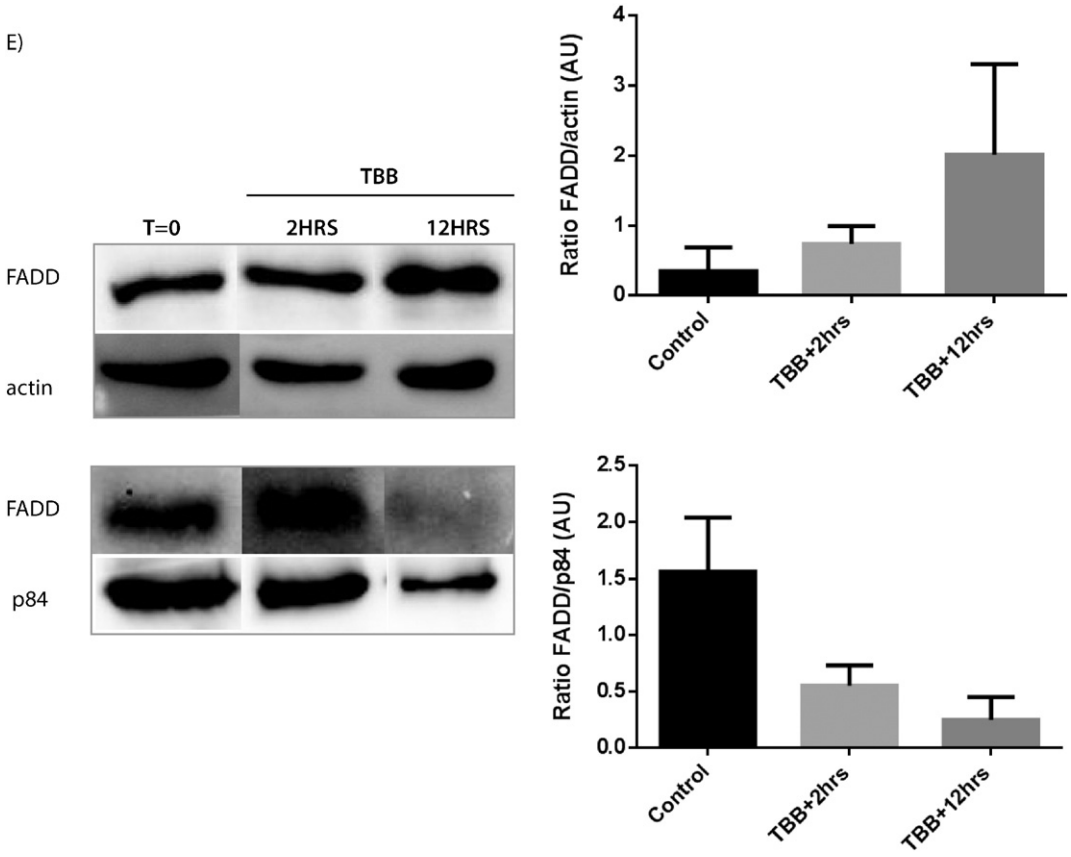

Fig.1 *(continued)*

Our results showed for the first time that CK2 binds and phosphorylates FADD in a CK2β dependent fashion. Blocking CK2 activity either with drugs or CK2β knockdown led to nuclear FADD loss and increased extracellular FADD. This regulation of FADD sub-cellular localization suggests that CK2 is a key component of the anti-apoptotic machinery to retain FADD in the nucleus and away from its pro-apoptotic partners.

2. Experimental procedures

2.1. Reagents

Brefeldin A, 4,5,6,7-Tetrabromo-2-azabenzimidazole (TBB), human recombinant FADD were purchased from Sigma (Sigma-Aldrich, Saint-Quentin Fallavier, France). CX4945 was synthesized by Cylene Pharmaceuticals (San Diego, CA, USA).

2.2. Cell culture

THP-1 cells were grown in RPMI 1640 (Invitrogen) supplemented with 10% fetal calf serum (The Cell Culture Company), 1% penicillin/streptomycin (Gibco-BRL, Life Technologies SAS, Saint Aubin, France), 5% sodium pyruvate (Gibco), 1% Hepes (Gibco) and maintained at 37 °C in a 5% CO_2 incubator. MCF10A cells were grown in DMEM-F12 Glutamax (Gibco) supplemented with 5% Horse serum, 0.025% EGF at 0.1 mg/ml, 0.05% hydrocortisone at 1 mg/ml (Sigma-Aldrich), 0.01% cholera toxin at 1 mg/ml (Sigma-Aldrich), 0.1% insulin at 10 mg/ml (Sigma-Aldrich) and 0.5% penicillin/streptomycin (Gibco).

2.3. Immunofluorescence staining

THP-1 cells were washed once in PBS and submitted to the cytospin technique (80,000 cells/spot) for efficient immunostaining. Cells were then fixed in 4% PFA for 30 min at RT, permeabilized in 0.05 M TBS pH 7.6 Triton 0.3% for 5 min at RT. The cells were then saturated in 10% horse serum in TBS for 20 min at RT. In order to visualize FADD, cells were incubated for 2 h at RT with anti-human FADD antibody (10 μg/ml) (Calbiochem, Merck Millipore, Molsheim, France) in 0.05 M TBS pH 7.6 followed by incubation with anti-rabbit IgG FITC-conjugated (10 μg/ml) (Santa Cruz Biotechnology, CA, USA). For triple staining of CK2α, CK2β and FADD, cells were incubated overnight with the respective antibodies (polyclonal αCOC antibody [34], monoclonal β-M and polyclonal anti-FADD) and for 1 h at RT with secondary antibodies (anti-rabbit FITC) (BD Pharmingen), anti-mouse Cy5 (Abcam, Paris, France), biotinylated anti-mouse + Streptavidin-PE (BD Pharmingen) respectively. To assess the concentration of nuclear FADD binary images were created and the mask option used. The signal given as an amount of pixel was indicative of FADD concentration in the nucleus; wt-MCF10A and ΔCK2β-MCF10A were grown overnight on lab-tek chamber slide (Nunc, Thermo-Fischer Scientific, Brebières, France), pre-coated for 6 h at 37 °C with polylysine. The cells were allowed to grow during 2 days before staining. Cells were then washed with PBS and stained with the appropriate antibodies. Cells were mounted in Vectashield Mounting Medium with DAPI (Vector Laboratories, Burlingame, CA, USA) and analyzed using a spinning disk confocal microscope (Leica) equipped with a CoolSnap HQ2 camera (Photometrics, Tucson, AZ, USA). Digital pictures were analyzed using MetaMorph 7 software (Molecular Devices, St-Grégoire, France) and processed using ImageJ software. For nuclear/cytoplasmic quantification of FADD, around 100–200 cells were counted for each condition and masks were created with ImageJ so that only the content of the nucleus was scored and compared between the control and the conditions treated with drugs. Colocalization of proteins is represented in white and was produced with the Colocalization Finder tool of ImageJ. Pearson's correlation coefficient was determined using the JaCoP plugin.

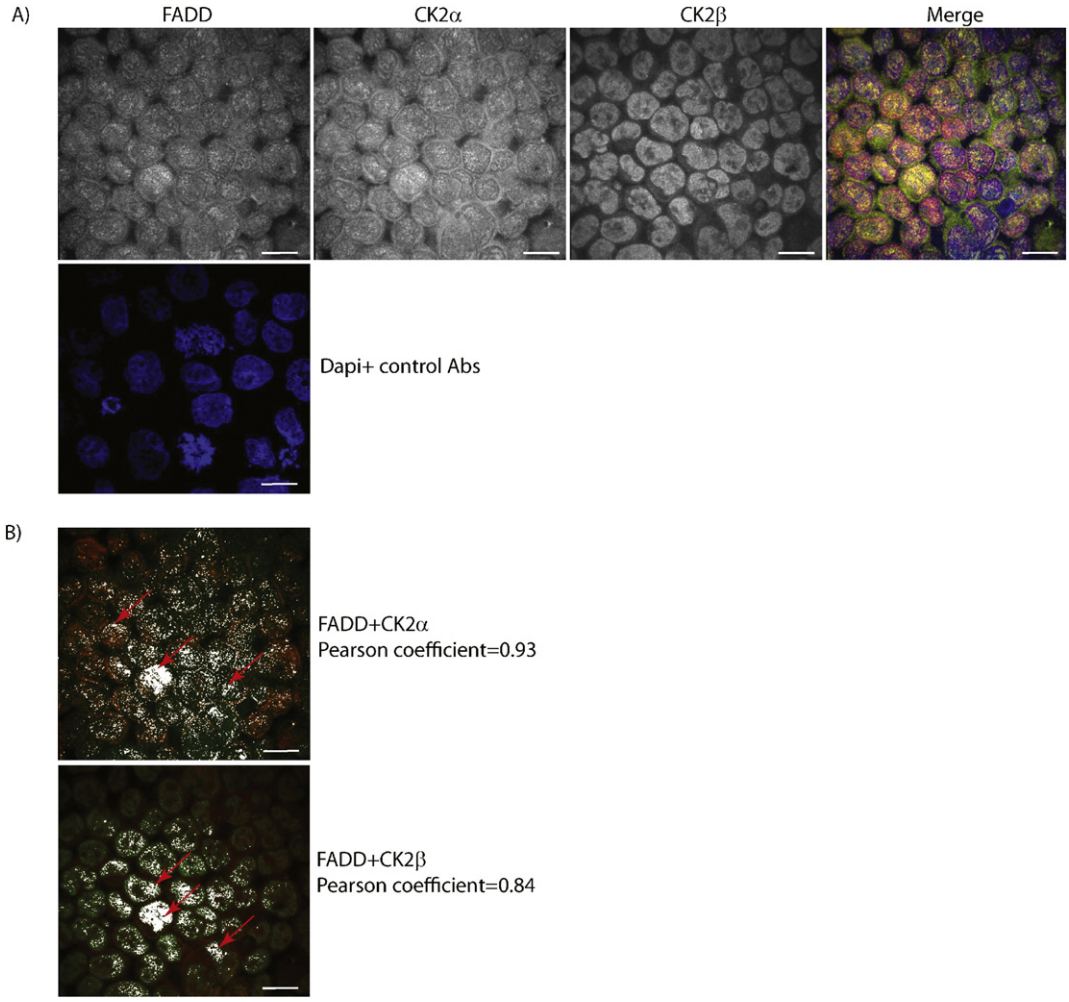

Fig. 2. Representative images of colocalization of FADD and CK2 subunits. A) THP-1 cells were fixed to slides following cytospin and were stained with anti-FADD pAb (green), anti-CK2α mAb (orange hot), anti-CK2β mAb (red) and DAPI (blue). B) Colocalization of FADD and CK2 subunits was assessed using the JaCoP plugin of ImageJ. Colocalized pixels are shown in white. Two independent experiments have been conducted. Five fields were counted per experiment, each field containing around forty cells. Pearson's correlation coefficients have been calculated on one representative merge images of FADD and CK2α or CK2β. Bars represent 10 μm.

2.4. In-vitro kinase assay

The kinase assay is based on phosphorylation of a CK2-specific peptide substrate using the transfer of the γ-phosphate of [γ-^{32}P] ATP by CK2 kinase as described in [35]. Recombinant CK2 subunits were expressed in bacteria and purified as described [46,47]. CK2 assays were performed using a specific CK2 peptide substrate as previously described [48]. MBP-FADD (2.5 μg) was incubated at 22 °C with 10 μM [γ-^{32}P] ATP and 10 mM $MgCl_2$ in the presence of 90 ng of either oligomeric CK2 or 50 ng of monomeric CK2α subunit supplemented with fixed (50 ng) or varying amounts (5–40 ng) of CK2β subunit. After 5 min, the reaction was stopped with 60 μl of 4% cold trichloroacetic acid. The proteins were precipitated for 30 min and the reaction mixture centrifuged. The supernatant was spotted on phosphocellulose paper and after 3 washes in cold 5% phosphoric acid, the radioactivity was counted in scintillation liquid.

2.5. Pull down assay

Extraction of THP-1 cells was done in normal lysis buffer (10 mM Tris–HCl, 150 mM NaCl pH 7.8, 1% Nonidet P-40). Prior to the pull down assay, Heparin-sepharose 6 Fast Flow column (GE Healthcare) were equilibrated in 50 mM Tris–HCl pH 7.5, 0.4 M NaCl, 1 mM DTT, 1% glycerol. THP-1 cell extracts were then loaded on the columns. The latter were washed (500 μl) with the equilibration buffer and CK2 was eluted with 300 μl of 50 mM Tris–HCl pH 7.5, 1.0 M NaCl, 1 mM DTT, 1% glycerol.

2.6. Protein extraction, dosage and Western blot

Proteins were extracted from cells using lysis buffer (10 mM Tris–HCl, 150 mM NaCl pH 7.8, 1% Nonidet P-40), containing a mixture of protease inhibitors (Complete, Mini, EDTA-free) (Roche Diagnostics, Meylan, France) and phosphatase inhibitors (PhosphoStop) (Roche Diagnostics). Protein concentration was determined using the Micro BCA Protein Assay Kit (Thermo Fischer Scientific) and/or the Nanodrop ND2000 (Thermo Fischer Scientific). Prior to immunoblot, 40 μg of protein extract was heated at 100 °C for 5 min in Laemmli buffer containing 2-β mercaptoethanol. Protein extracts (40 μg/lane) were then separated by SDS-PAGE at 25 mA and transferred to polyvinyledineflouride (PVDF) membranes by electroblotting at 125 V for 1 h. The membrane was then blocked with TBS 0.1% Tween 20, 5% non-fat dry milk at 37 °C for 60 min. After blocking, the membrane was washed once with TBS (5 min), probed with anti-hFADD BD Pharmingen (1:250 in TBS 0.1% Tween 20, 5% non-fat dry milk) and incubated at 37 °C for 60 min. The membrane was then washed with TBS 0.1% Tween (3 × 5 min), followed by addition of affinity-purified

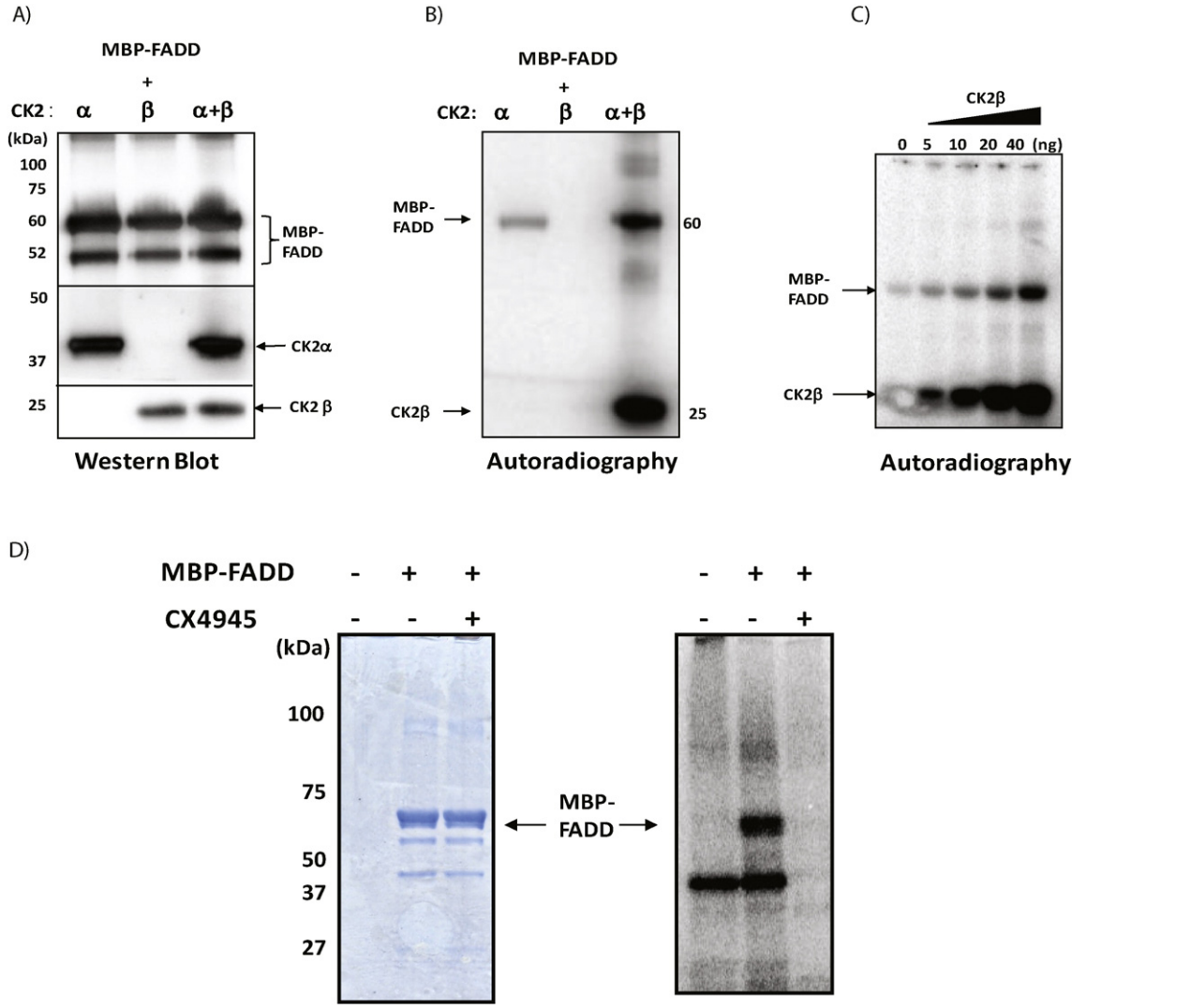

Fig. 3. CK2 directly binds and phosphorylates FADD. A) Western blotting of FADD and CK2 subunits. B) In-vitro kinase assay was performed using 2.5 μg of MBP-FADD, recombinant CK2 subunits (50 ng of CK2α and 40 ng of CK2β) or recombinant holoenzyme (90 ng) and [γ-^{32}P] ATP and 10 mM $MgCl_2$. Reaction mixture was transferred to phospho-cellulose paper and phosphorylation of MBP-FADD was detected by autoradiography. C)Variable concentrations of CK2β (5–40 ng) were used to evaluate the necessity of the regulatory subunit in FADD phosphorylation. D) CK2 was pulled-down from THP-1 cell extract using heparin-sepharose columns. The columns were washed and CK2 was recovered in elution buffer (see Materials and methods). The resulting CK2 was used for in-vitro kinase assay performed on MBP-FADD (same conditions as above) in the presence or absence of CX-4945. Phosphorylation was detected with autoradiography.

anti-mouse IgG conjugated to horseradish peroxidase Dako Cytomation (1:10,000 in TBS 0.1% Tween 20, 5% non-fat dry milk) and incubated at 37 °C for 60 min. After incubation, the membrane was washed with TBS 0.1% Tween 20 (3 × 5 min). The membrane was then incubated 1 min in ECL Prime solution (Amersham, GE Healthcare Europe GmbH, Velizy-Villacoublay, France) and the chemoluminescent signal revealed with the image acquisition system Fusion FX7 (Vilber Lourmat).

2.7. Identification of CK2 phosphorylation site in FADD

To determine the phosphorylation site, 3 μg of MBP-FADD was phosphorylated by CK2 in the presence or absence of 100 μM ATP-$MgCl_2$. Proteins were resolved by SDS-PAGE and were stained with Coomassie blue. Gel bands from MBP-FADD were excised and cut in pieces. The following sample incubations were performed automatically using a Freedom EVO150 robot (Tecan Traging AG, Switzerland). Gel pieces were washed by 6 successive incubations of 15 min in 25 mM NH_4HCO_3 and in 25 mM NH_4HCO_3 containing 50% (v/v) acetonitrile. Gel pieces were then dehydrated with 100% acetonitrile and incubated for

Table 1
CK2 putative sites in FADD. Summary of the 14 CK2 putative sites identified in FADD by the HPRD (Human Protein Reference Database). Potential phosphorylated serines are in bold.

	Position in query protein	Sequence in query protein
1	10	**S**VS
2	14	**S**LS
3	16	**S**SSE
4	17	**S**SE
5	18	**S**ELT
6	41	**S**GLD
7	122	**S**DT
8	124	**T**KID
9	128	**S**IE
10	151	**T**EKE
11	194	**S**PMS
12	200	**S**DAS
13	203	**S**TSE
14	205	**S**EAS

Table 2
Identification of a phosphorylatable peptide by MS/MS. A 19 amino-acid long peptide SGAMSPMSWNSDASTSEAS was identified by MS/MS analysis. For all the queries with a number 1 rank (99.61%, 94.38%, 64.66% respectively) showed in bold, the peptide was phosphorylated on serine 200 (Sp).

Query number	Rank	Peptide score	Peptide sequence	Peptide modification	Probability assignation
2698	**1**	**74.12**	**SGAMSPMSWNSpDASTSEAS**	**Phospho (ST)**	**99.61%**
2736	**1**	**33.12**	**SGAMoxSPMSWNSpDASTSEAS**	**Oxidation (M); Phospho (ST)**	**64.66%**
2736	2	25.96	SGAMoxSPMSpWNSDASTSEAS	Oxidation (M); Phospho (ST)	12.44%
2736	3	24.91	SGAMoxSPMSWNSDASpTSEAS	Oxidation (M); Phospho (ST)	9.76%
2736	4	21.34	SGAMoxSPMSWNSDASTpSEAS	Oxidation (M); Phospho (ST)	4.29%
2736	5	20.01	SGAMSPMoxSWNSpDASTSEAS	Oxidation (M); Phospho (ST)	3.16%
2736	6	15.12	SGAMoxSpPMSWNSDASTSEAS	Oxidation (M); Phospho (ST)	1.02%
2752	**1**	**52.62**	**SGAMoxSPMoxSWNSpDASTSEAS**	**2 Oxidation (M); Phospho (ST)**	**94.38%**
2752	2	37.29	SGAMoxSPMoxSpWNSDASTSEAS	2 Oxidation (M); Phospho (ST)	2.77%
2752	3	34.89	SGAMoxSPMoxSWNSDASpTSEAS	2 Oxidation (M); Phospho (ST)	1.59%
2752	4	33.32	SGAMoxSPMoxSWNSDASTpSEAS	2 Oxidation (M); Phospho (ST)	1.11%

45 min at 53 °C with 10 mM DTT in 25 mM NH_4HCO_3 and for 35 min in the dark with 55 mM iodoacetamide in 25 mM NH_4HCO_3. Alkylation was stopped by adding 10 mM DTT in 25 mM NH_4HCO_3 and mixing for 10 min. Gel pieces were then washed again by incubation in 25 mM NH_4HCO_3 before dehydration with 100% acetonitrile. 0.5 μg of modified trypsin (Promega, sequencing grade) in 25 mM NH_4HCO_3 was added to the dehydrated gel pieces for an overnight incubation at 37 °C. Peptides were then extracted from gel pieces in three 15 min sequential extraction steps in 30 μl of 50% acetonitrile, 30 μl of 5% formic acid and finally 30 μl of 100% acetonitrile. The pooled supernatants were then dried under vacuum. The dried extracted peptides were resuspended in 5% acetonitrile and 0.1% trifluoroacetic acid and analyzed by online nanoLC-MS/MS (Ultimate 3000, Dionex and LTQ-Orbitrap Velos pro, Thermo Fischer Scientific). The nanoLC method consisted in a 30-minute gradient ranging from 4% to 45% acetronitrile in 0.1% formic acid at a flow rate of 300 nL/min. Peptides were sampled on a 300 μm × 5 mm PepMap C18 precolumn and separated on a 75 μm × 250 mm C18 PepMap column (Thermo Fischer Scientific). MS and MS/MS data were acquired using Xcalibur (Thermo Fischer Scientific). Survey full-scan MS spectra ($m/z = 400–1600$) were acquired in the Orbitrap operated in positive mode with a resolution of 60,000 after accumulation of 10^6 ions (maximum filling time: 500 ms). The fifteen most intense ions were selected for fragmentation by multi stage activation after accumulating ions to a target value of 5000 and a max. injection time of 100 ms. Data were automatically processed using Mascot Daemon software (version 2.3, Matrix Science). Peak lists were generated with Mascot Distiller version 2.3.2.0 software (Matrix Science) from the LC-MS/MS raw data. Searches against a homemade database containing FADD and MBP sequences and against contaminants database (658 sequences in total for these 2 databases) and the corresponding reversed databases were performed using Mascot (version 2.4). ESI-FTICR was chosen as the instrument, semitrypsin as the enzyme and 2 missed cleavage allowed. Precursor and fragment mass error tolerances were set respectively at 5 ppm and 1 Da. Peptide modifications allowed during the search were as follows: carbamidomethylation (C, fixed) acetylation (protein N-term, variable), oxidation (M, variable) and phosphorylation (S, T, Y, variable [36]). The IRMa software (version 1.31.1) was used to filter results. Peptides with a Mascot score above 30 were validated. Protein groups identified with two different peptides and at least one proteotypic peptide were furthermore validated.

2.8. Site directed mutagenesis

Site directed mutagenesis was performed using the QuickChange II XL Site-Directed Mutagenesis Kit according to the manufacturer's protocol. Serine 200 was replaced by an alanine. Fwd primer: CCCCGA TGTCATGGAACGCAGACGCATCTACCTCC and rev primer: GGAGGTAG ATGCGTCTGCGTTCCATGACATCGGGG were used (underlined is the modified amino acid sequence).

2.9. Plasmid vectors and transfection

The plasmid vector FADD-FLAG was kindly provided by Pr. Astar Winoto (Division of Immunology and Pathogenesis, Department of Molecular and Cell Biology, University of California, Berkeley, California, USA). THP-1 cells were transfected with the FADD-FLAG using the AMAXA kit V for immunoprecipitation assays and with the FADD-FLAG/FADD-FLAG S200A with the Lipofectamine 2000 kit (Invitrogen) for immunofluorescence assays according to the manufacturers.

2.10. Statistical analysis

Statistical significance was determined using Mann–Whitney non parametric test or two-way ANOVA for multiple group analysis where necessary. $p \leq 0.05$ was considered as significant.

3. Results

3.1. Nuclear FADD decreases after inhibition of CK2 activity

Given the importance of FADD sub-cellular localization on its cellular activities, we searched for possible regulatory mechanisms involved in its nuclear redistribution and restriction. While screening for regulatory partners, we investigated the role of the protein kinase CK2, which is already known to regulate proteins involved in the apoptotic process [31,32]. We examined FADD localization in the myelomonocytic cell line, THP1, in conditions where CK2 kinase activity was inhibited. We carried out confocal microscopy experiments to investigate the localization of endogenous FADD in resting and TBB-treated THP-1 cells. TBB is a cell permeant highly selective, ATP/GTP-competitive inhibitor of casein kinase-2 which binds to Val66 in the hydrophobic pocket, precluding thereafter the binding of CK2 to ATP/GTP [37]. In non-treated cells, FADD was localized mainly in the nucleus (Fig. 1A panel a). At each time point following treatment with TBB (2 h, 12 h and 14 h), cells were washed and labeled with FADD antibody and DAPI. We observed a significant decrease of nuclear FADD concentration upon treatment with TBB as observed after 14 h of TBB treatment (Fig. 1A panel b). Quantification results confirmed that nuclear FADD dropped off in presence of TBB as observed with the significant decrease between the control and treated conditions (Fig. 1B). We did the same experiments with CX-4945, a more specific CK2 inhibitor. Again, nuclear FADD decreased strongly (Fig. 1C panels a–c). Quantification studies

Fig. 4. CK2 phosphorylates FADD on serine 200. A) Comparison of the cumulated mass spectrum over the chromatographic elution peak of SGAMSPMSWNSpDASTSEAS between the unphosphorylated and phosphorylated sample. The zoom corresponds to the mass range of 985–1000 m/z. B) Comparison of extracted ion chromatogram for the peptide SGAMSPMSWNSpDASTSEAS over the entire LC gradient between the non-phosphorylated and phosphorylated samples. Arrows in bold represent peaks corresponding to phosphorylated peptide. c) Phylogenetic tree and partial sequences enclosing the conserved serine 200 residue in different species.

A)

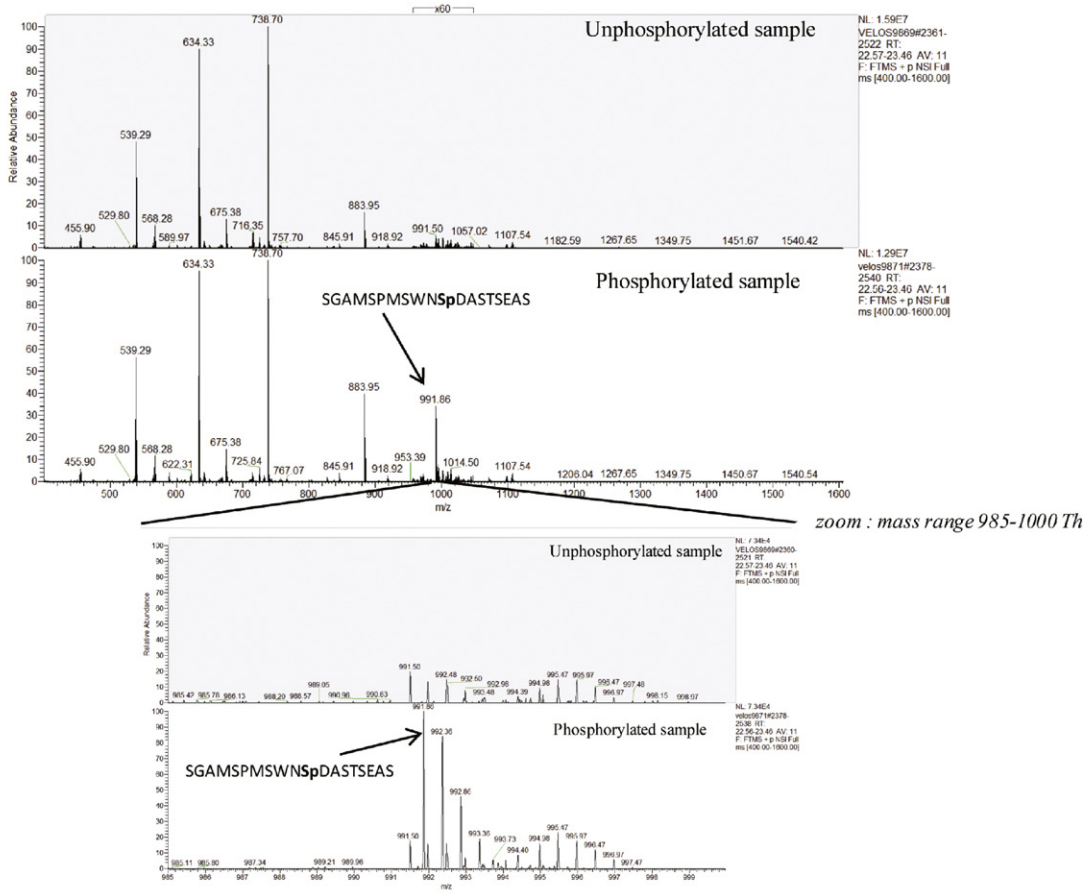
Unphosphorylated sample
Phosphorylated sample
SGAMSPMSWNSpDASTSEAS
zoom : mass range 985-1000 Th
Relative Abundance
m/z

B)

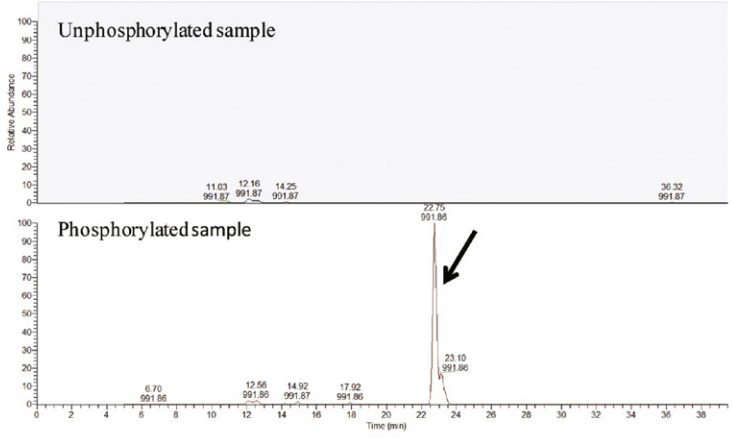
Unphosphorylated sample
Phosphorylated sample
Relative Abundance
Time (min)

C)

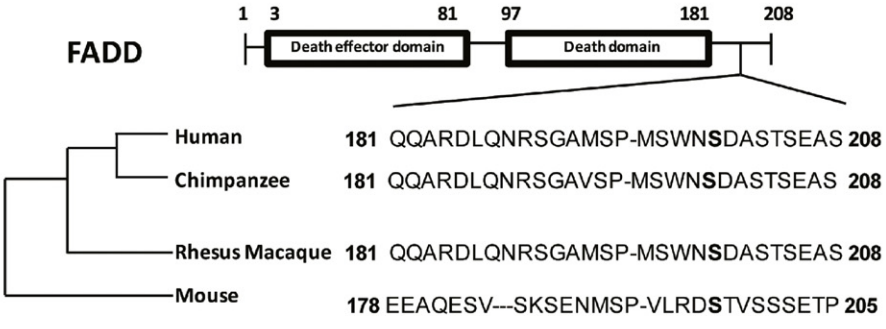
FADD
1 3 81 97 181 208
Death effector domain
Death domain
Human 181 QQARDLQNRSGAMSP-MSWNSDASTSEAS 208
Chimpanzee 181 QQARDLQNRSGAVSP-MSWNSDASTSEAS 208
Rhesus Macaque 181 QQARDLQNRSGAMSP-MSWNSDASTSEAS 208
Mouse 178 EEAQESV---SKSENMSP-VLRDSTVSSSETP 205

substantiated the results obtained with TBB. In fact, at the two time points studied, there was a significant decrease in nuclear FADD after 2 h and 4 h of CX-4945 treatment (Fig. 1D—a and b). To support the data obtained with immunofluorescence studies, subcellular fractionation of THP-1 cells were performed. THP-1 cells were treated with TBB and protein extracts were prepared at the indicated time points and resolved on SDS-PAGE. Ratio of FADD to cytoplasmic (actin) or nuclear (p84) loading controls are given as arbitrary units. The results show that there is an increase of FADD/actin ratio over time while a parallel decrease in the FADD/p84 ratio is observed (Fig. 1E, Supplemental Fig. 1). Collectively, these results demonstrate that inhibition of CK2 activity induced a significant decrease of nuclear FADD and suggest that in THP-1 cells, CK2 activity could be necessary to restrict or to maintain FADD localization inside the nucleus.

3.2. CK2 subunits and FADD colocalize into the nucleus

To understand whether the observed change in FADD distribution upon CK2 inhibition could be explained by a direct interaction between FADD and CK2, we conducted colocalization studies. It has been documented that CK2α and β subunits can be localized in the cytoplasm and the nucleus, together or separately [38]. How, why and where the CK2 subunits will interact is still under investigation [39]. In THP-1 cells, the regulatory and catalytic subunits of CK2 were localized in both the cytoplasm and the nucleus albeit with a higher concentration in the latter (Fig. 2A). In the merge pictures, colocalized pixels, in white, showed that CK2 subunits and FADD colocalized exclusively in the nucleus (Fig. 2B). The calculation of Pearson's correlation coefficient using the JaCoP plugin of ImageJ gave rise to high r values (0.93 for FADD/CK2α and 0.84 for FADD/CK2β) (Fig. 2B). We carried out the same experiments in Jurkat T lymphocytes cell line and observed a similar nuclear colocalization of FADD and CK2 subunits (data not shown). This colocalization raised the possibility that FADD and CK2 might interact as a molecular complex in living cells.

3.3. FADD is phosphorylated by the CK2 holoenzyme in a CK2β-dependent manner

In light of the above results we investigated whether CK2 could bind and phosphorylate FADD in vitro using recombinant CK2 subunits and recombinant FADD (MBP-FADD). To determine whether CK2 subunits bind directly to FADD, we performed in vitro binding assays. CK2α or CK2β either individually or mixed together were incubated with amylose beads loaded with MBP-FADD. Western blot analysis using anti-MBP antibody showed that the MBP-FADD bound to both CK2 subunits (Fig. 3A). When CK2α or CK2β were mixed together to generate the holoenzyme prior to incubation with MBP-FADD, a similar amount of both CK2 subunits bound to the fusion protein indicating that in vitro, both CK2 subunits interact with FADD individually (Fig. 3A). To investigate whether or not CK2 could phosphorylate FADD in vitro, MBP-FADD was incubated with CK2α or CK2β individually or with the holoenzyme in the presence of [γ-^{32}P]ATP/Mg. As shown in Fig. 3B MBP-FADD was weakly phosphorylated by the isolated CK2α subunit whereas its phosphorylation was strongly enhanced in the presence of the holoenzyme. The 27 kDa band corresponded to autophosphorylation of the CK2β subunit in the holoenzyme complex [24]. We noticed that only the higher form of the FADD protein at 60 kDa could be phosphorylated. Given that MBP-FADD was bound to maltose resin for the in vitro kinase assay, phosphorylation could take place only on the C-terminal part of the recombinant protein. Furthermore, phosphorylation was potentiated with increasing concentrations of the CK2β subunit and optimal phosphorylation was observed in the presence of stoichiometric amounts of CK2 catalytic and regulatory subunits, thereby showing that FADD phosphorylation is a CK2β driven process (Fig. 3B and C). We also verified whether endogenous CK2, like recombinant CK2, could bind and phosphorylate FADD. The polyanionic structure of heparin allowed recovering CK2 kinase from the extracts [40]. Therefore, we carried out heparin-sepharose affinity chromatography to pull-down the endogenous CK2 from THP-1 extracts and assess its capacity to phosphorylate recombinant FADD. In these conditions, recombinant FADD was also readily phosphorylated (Fig. 3D). Moreover, when the phosphorylation assay was carried out in the presence of CX-4945, FADD was not phosphorylated anymore indicating that endogenous CK2 served as a kinase for FADD phosphorylation. We obtained the same results with CK2 brought down from Jurkat extract (Supplemental Fig. 2). Thus, these results demonstrate that the CK2 tetrameric holoenzyme might be a FADD kinase.

3.4. CK2 phosphorylates FADD on serine 200

Basic primary sequence analysis identified fourteen potential CK2 phosphorylation sites on human FADD protein (Table 1). To determine the actual phosphorylation sites, we used tandem mass spectrometry (MS/MS) experiments. We incubated MBP-FADD with recombinant CK2 holoenzyme in the absence or presence of ATP-$MgCl_2$. The proteins were purified on SDS-PAGE and related bands were excised and digested with trypsin. Resulting peptides mixtures were separated by online reversed-phase nanoscale capillary LC and analyzed by ESI-MS/MS. Confrontation of MS/MS spectra to protein databases by Mascot software led to the identification of FADD with more than 70% of sequence coverage for both unphosphorylated and phosphorylated samples. While for the unphosphorylated sample, no spectrum was validated for any phosphorylated peptide, three spectra corresponding to different oxidized forms of the same phosphorylated peptide SGAMSPMSWNSDASTSEAS (from amino acid 190 to 208) were validated for the phosphorylated sample. As this peptide shows eight different possible phosphorylation sites, we used site analysis based on Mascot delta score [41] to correctly assign the phosphorylation site. The different probabilities corresponding to the possible site assignations are reported in Table 2 for each spectrum. Phosphorylation could be localized to the serine 200 with high probability for two of these spectra (99.6% and 94.4%). Last spectrum gave same assignation but with a lower probability. To confirm the specificity of the CK2 activity and of the identified phosphorylated peptide, we extracted the different masses of its three forms from the chromatogram. Extracted ion chromatogram of the non-oxidized form (m/z 991.86Th) showed that this peptide is detected only in the phosphorylated sample (Fig. 4A). Moreover, as shown on the mass spectrum cumulated over the elution peak of this peptide (22.56–23.46 min), no ion corresponding to the above peptide was detected in the unphosphorylated sample even with a low intensity compared to the phosphorylated sample (Fig. 4B). Comparison of hFADD protein sequence and non-human primates and mouse FADD sequence showed that the serine 200 is conserved, suggesting that this CK2-dependent FADD nuclear restriction mechanism could be conserved in other organisms (Fig. 4C).

3.5. Serine 200 is required for FADD nuclear retention

To test that S200 phosphorylation is necessary for FADD retention in the nucleus, we observed the localization of FADDS200A in THP-1 cells. Site directed-mutagenesis was performed and plasmids bearing either FADD-FLAG (FADDwt) or FADD200A-FLAG were used to transfect THP-1 cells and followed by immunofluorescence to detect localization of FADDwt and FADDS200A. We observed that, as expected, FADD-FLAG showed nuclear and cytoplasmic expression with a very high bias towards nuclear expression as we had seen for endogenous FADD (Fig. 5A). FADD S200A showed high cytoplasmic expression (Fig. 5B). In fact, FADD seemed to be nearly completed excluded from the nucleus suggesting that serine 200 is important for nuclear retention of FADD.

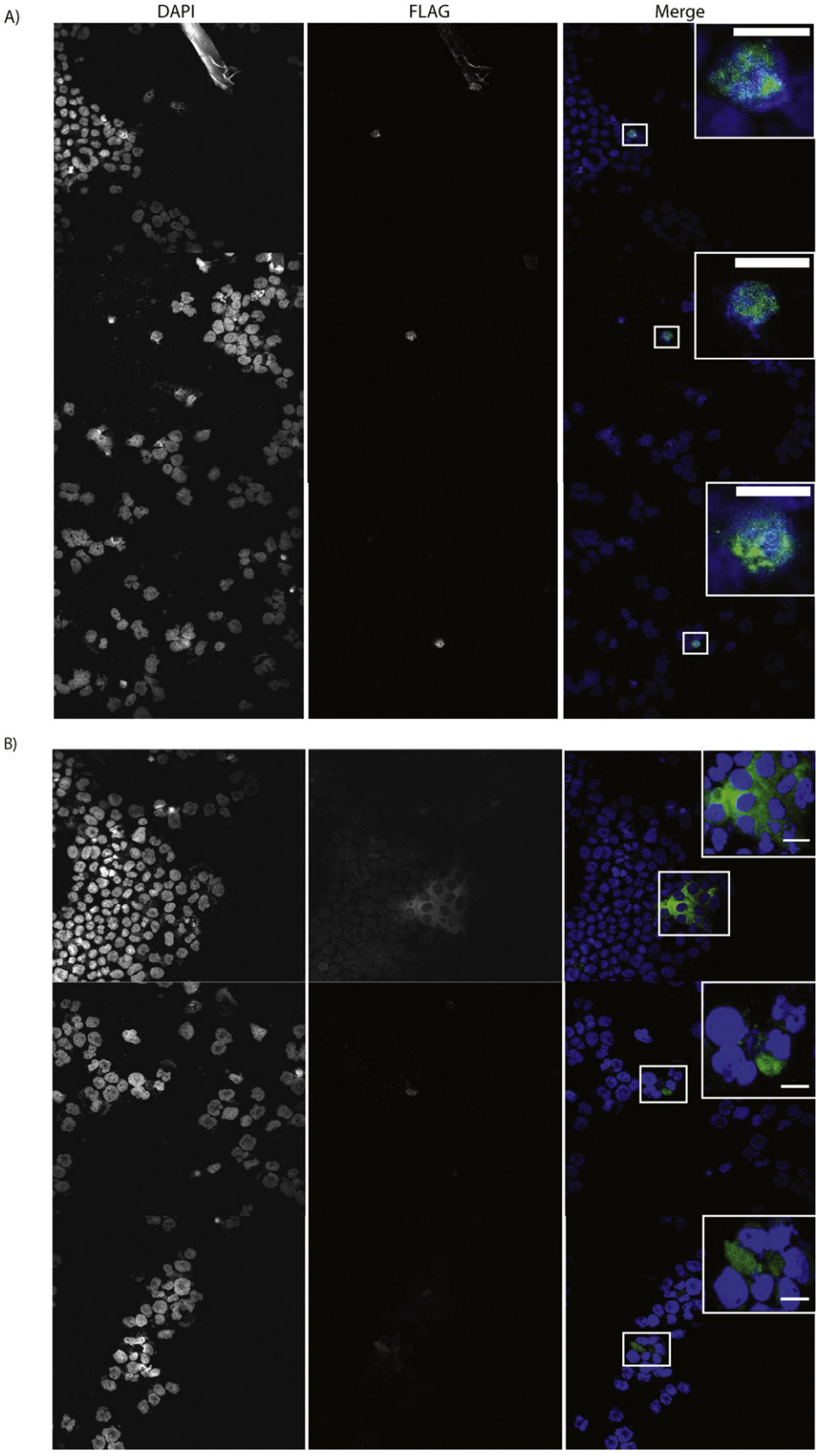

Fig. 5. Representative montages of comparison between FADD-FLAG (FADDwt) and FADD-S200A sub-cellular localizations in THP-1 cells. The cells were transfected with FADD-FLAG or FADD-S200A and labeled as follows: anti-FLAG pAb (green) and DAPI (blue). The montage show transfected FADD-FLAG (A) and FADD-S200A (B) cells from different experiments. Bars in the inset represent 20 μm.

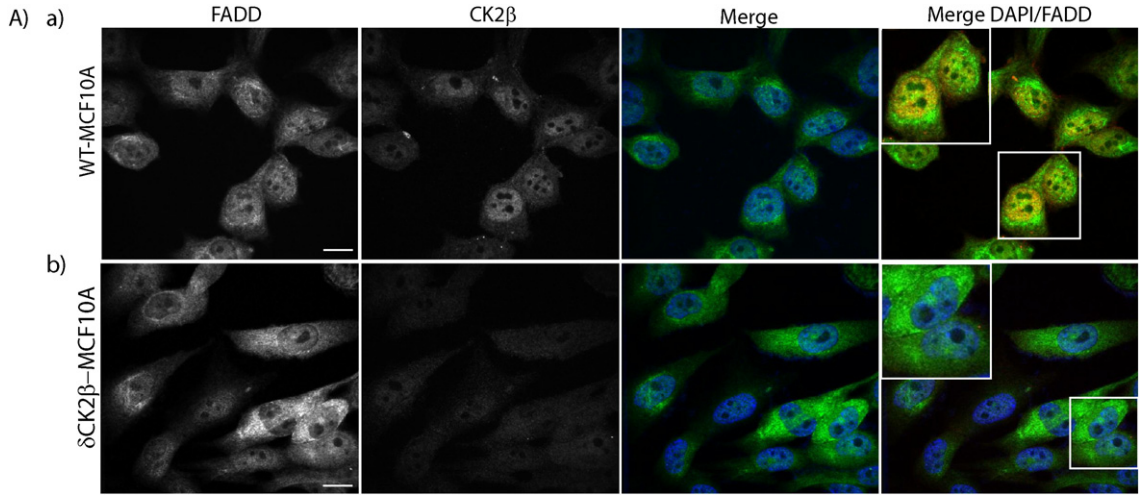

Fig. 6. Representative images of comparison between FADD sub-cellular localizations in MCF10A-wt and MCF10A-ΔCK2β. Cells were grown on lab-tek slides and labeled as follows: anti-FADD pAb (green), anti-CK2β mAb (red) and DAPI (blue). Two independent experiments were conducted. Thirty-two fields have been counted per experiment, each field containing around fifteen cells. Sections of each overlay images are magnified. Bars represent 15 μm.

3.6. Downregulation of the CK2β regulatory subunit results in nuclear FADD loss

Since the presence of CK2β is crucial for FADD phosphorylation, we used an immortalized human breast epithelial cell line, MCF10A-ΔCK2β, in which expression of CK2β has been knocked down [42]. FADD localization was analyzed in MCF10A-*wt* and MCF10A-ΔCK2β cells by confocal microscopy. As previously described by Screaton et al. [18] FADD was localized mainly in the nucleus of the MCF10A-*wt* (Fig. 6A). Similarly, CK2β was concentrated in the nucleus of the MCF10A-*wt* (Fig. 6A). However, in MCF10A-ΔCK2β cells, the localization of FADD was clearly shifted to the cytoplasm though some FADD was also detected in the nucleus (Fig. 6B, see magnification). As expected, the signal was null for CK2β (Fig. 6B). Merge of DAPI and FADD disclosed that in conditions where CK2β expression was downregulated, nuclear FADD was lost. These results corroborated the results obtained in TBB- or CX-4945-treated THP-1 cells in which CK2 activity was dramatically reduced. Given the requirement of CK2β for optimal FADD phosphorylation, conditions found in MCF10A-ΔCK2β cells mimicked somehow the effect observed in response to drug-induced inhibition of CK2 catalytic activity. As already observed [42] CK2α was concentrated in the nucleus of MCF10A-*wt* cells whereas the protein was mainly cytoplasmic for MCF10A-ΔCK2β cells (data not shown). These results clearly suggested that CK2 activity might play a role for nuclear localization of FADD.

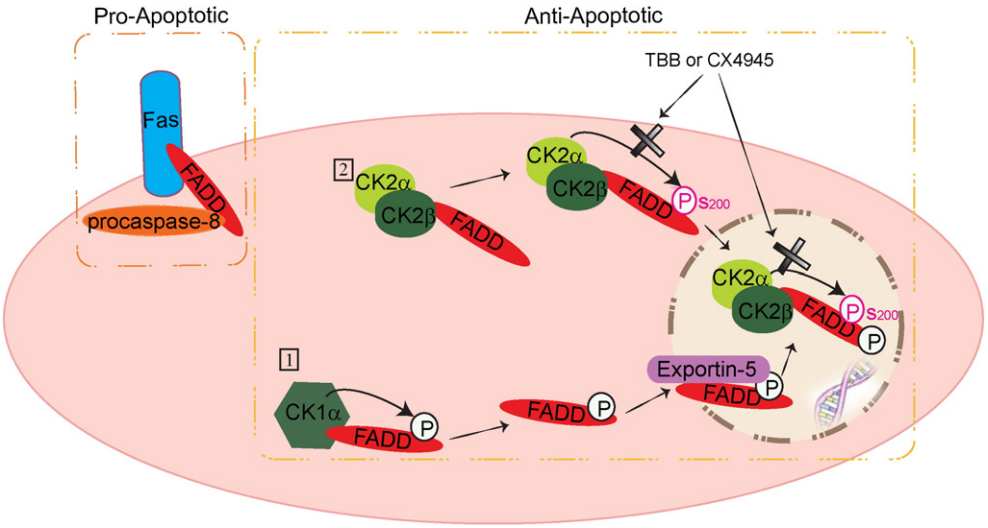

Fig. 7. Schematic diagram of phosphorylation of FADD by the anti-apoptotic protein kinase CK2 and its effect on FADD sub-cellular localization. In the cytoplasm, FADD can act as a pro-apoptotic protein upon its binding with the death receptor Fas and pro-caspase-8. Regarding FADD nuclear localization, two scenarios could be possible: 1) Phosphorylation of FADD by CK1α, occurring in the cytoplasm, has already been described. This phosphorylation will allow FADD to be shuttled from the cytoplasm to the nucleus via Exportin-5 dependent mechanism. Once, in the nucleus, FADD could bind to the CK2 holoenzyme, be further phosphorylated by CK2α on serine 200 and retained in the nucleus where it would act as an anti-apoptotic factor or 2) FADD could bind to the CK2 holoenzyme in the cytoplasm first. CK2α would phosphorylate FADD on serine 200 and the whole complex would shuttle to the nucleus where it would be retained and would act as an anti-apoptotic factor. TBB or CX4945 treatment will inhibit CK2, precluding FADD phosphorylation in the cytoplasm or the nucleus. In such circumstances, FADD would not be retained anymore in the nucleus and would augment in the cytoplasm.

4. Discussion

In an attempt to identify possible regulators of FADD sub-cellular localization we identified the anti-apoptotic kinase CK2 as a key actor. We demonstrated for the first time that CK2 activity influences FADD localization (Fig. 1A–E) and that CK2 colocalizes with, binds and phosphorylates FADD in vitro (Fig. 2A, B, Fig 3A-C). It has previously been reported as data not shown that recombinant CK2 could not phosphorylate FADD [19]. One possibility to explain such discrepancy is that the material and conditions used for the in vitro kinase assay might have been detrimental somehow and did not allow for identification of phosphorylated FADD. One important observation is that optimal phosphorylation was observed in the presence of stoichiometric amounts of CK2 catalytic and regulatory subunits, thereby showing that FADD phosphorylation is a CK2β driven process. Several studies have shown that some substrates could be phosphorylated by CK2α alone as it is spontaneously active [26]. However, the CK2 regulatory subunit requirement for efficient CK2-mediated FADD phosphorylation is of interest since it has been reported that CK2β could serve as a scaffold or docking platform to enhance the affinity of CK2α for its substrate [26,43]. Therefore, FADD belongs to the growing list of CK2β-dependent substrates. Importantly, endogenous CK2 isolated from THP-1 extracts (Fig. 3D) as well as Jurkat cell extracts (data not shown) were efficient for in vitro phosphorylation of recombinant FADD (Fig. 3D) and this phosphorylation was alleviated by the presence of CX-4945, the actual most specific CK2 inhibitor. Of note, the CX-4945 is in a phase II clinical trial in patients suffering of remitting multiple myelomas [44].

It is largely accepted that FADD requires nuclear positioning to carry out its non-apoptotic functions [17]. It has been very elegantly demonstrated by Alappat et al. that phosphorylation of FADD by CK1α on serine 194 is essential for FADD nuclear localization. It is currently unclear whether FADD is phosphorylated first and then sent to the nucleus or whether FADD travels to the nucleus via binding to CK1α and undergoes post-translational modifications once there [17]. Herein, we brought evidence that FADD phosphorylation by CK2 might be important to keep FADD in the nucleus. Under conditions where CK2 activity was hampered either by pharmacological means or by CK2β subunit expression knock-down, nuclear FADD was strongly decreased (Fig. 6). It is known that FADD is not located similarly in all cell lines. How important is the role of CK2 in every type of cells regarding FADD sub-cellular localization is beyond the scope of this report. The fact that co-localization of FADD and CK2 was restricted to the nucleus is of significance since a large number of CK2 substrates are found in the nucleus and many of these are usually DNA/RNA structural proteins and transcription factors [39]. It is known that nuclear CK2 is correlated with apoptosis resistance which might be reminiscent of a potential role of CK2 in FADD anti-apoptotic activities [29]. We found that in condition where TBB is added to THP-1 cells, the latter showed a higher sensitivity to cell death (unpublished). We found the same results in MCF10A-ΔCK2β. These results are in line with our data that CK2, once inhibited could cause nuclear FADD loss and therefore potentially more FADD at the death inducing signaling complex (DISC). However we cannot rule out the possibility that other functions of CK2, independently of its effect on FADD, might cause increased cell death in condition of inhibition. Evidence has shown that FADD can bind to MBD-4 protein in the nucleus [18] and thus participate in genome surveillance through a mechanism which still needs to be understood. Such a mechanism might be involved in a CK2-driven FADD anti-apoptotic activity or along this line, a mechanism which might recruit CK2, FADD as well as MBD-4.

Serine 200 was identified by mass spectrometry analysis identified as the actual phosphorylation site of CK2 in the FADD protein (Fig. 4A, B, Table 2). This residue does not lie within a S/T-X-X-D/E canonical CK2 phosphorylation site (Table 1), where X might be any residue and where the most important residue is the acidic residue at n + 3. However, while a majority of the proteins phosphorylated by CK2 have an acidic residue at n + 3, the second most important position is the presence of an acidic residue at n + 1 [25] like in the case of FADD therefore reinforcing the accuracy of the identified serine. Phylogenetic comparison showed that this serine is conserved not only among higher primates but also in mice suggesting a possible important role for this residue in FADD regulation (Fig. 4C). Mass spectrometry analysis were reinforced by site-directed mutagenesis. Indeed FADDS200A abolished the function of CK2 on FADD nuclear localization (Fig. 5B). These data are consistent with the conservation of the serine 200 during evolution.

We therefore propose a possible scheme whereby CK1 binding and phosphorylation of FADD would allow the latter to enter the nucleus. Once there, further phosphorylation by CK2 could lead to sequestering of FADD inside this organelle in order to keep it away from the death receptors thus down-regulating apoptosis (Fig. 7).

In conclusion, our results show for the first time a molecular interaction between CK2 and FADD and we suggest that this interaction could play a role in FADD nuclear localization. Perspective work would be required to identify whether a possible dialogue could exist between CK1- and CK2-mediated phosphorylation of FADD and to dig further the significance of this interaction to the cell processes. While our data show that FADD is phosphorylated on serine 200 by the CK2 kinase, we still don't know where, within the cell, the phosphorylation process occurs.

Supplementary data to this article can be found online at http://dx.doi.org/10.1016/j.bbamcr.2015.08.001.

Conflict of interest

The authors declare no conflict of interest.

Acknowledgments

We greatly acknowledge Pierre Bourdoncle, Béatrice Durel and Thomas Guilbert of the Cochin Imaging facility for the help with photonic microscopy. We thank François Guilloneau, Virginie Salnot and France Lam of the Paris Descartes Proteomic facility for technical assistance. We thank Dr. Claudine André and Dr. Matthieu Giraud for helpful discussion. Part of this work has been supported by La Ligue Contre le Cancer (TDEJ1433), Comité de Paris and by the Arthritis Foundation (2011-2013).

References

[1] A.M. Chinnaiyan, K. O'Rourke, M. Tewari, V.M. Dixit, Cell 81 (1995) 505–512.
[2] P.M. Chaudhary, M. Eby, A. Jasmin, A. Bookwalter, J. Murray, L. Hood, Immunity 7 (1997) 821–830.
[3] P. Schneider, M. Thome, K. Burns, J.L. Bodmer, K. Hofmann, T. Kataoka, N. Holler, J. Tschopp, Immunity 7 (1997) 831–836.
[4] W. Schneider-Brachert, V. Tchikov, J. Neumeyer, M. Jakob, S. Winoto-Morbach, J. Held-Feindt, M. Heinrich, O. Merkel, M. Ehrenschwender, D. Adam, R. Mentlein, D. Kabelitz, S. Schutze, Immunity 21 (2004) 415–428.
[5] A.M. Chinnaiyan, K. O'Rourke, G.L. Yu, R.H. Lyons, M. Garg, D.R. Duan, L. Xing, R. Gentz, J. Ni, V.M. Dixit, Science 274 (1996) 990–992.
[6] L. Tourneur, G. Chiocchia, Trends Immunol. 312010 260–269.
[7] W.C. Yeh, J.L. Pompa, M.E. McCurrach, H.B. Shu, A.J. Elia, A. Shahinian, M. Ng, A. Wakeham, W. Khoo, K. Mitchell, W.S. El-Deiry, S.W. Lowe, D.V. Goeddel, T.W. Mak, Science 279 (1998) 1954–1958.
[8] J. Zhang, D. Cado, A. Chen, N.H. Kabra, A. Winoto, Nature 392 (1998) 296–300.
[9] J. Zhang, N.H. Kabra, D. Cado, C. Kang, A. Winoto, J. Biol. Chem. 276 (2001) 29815–29818.
[10] K. Newton, A.W. Harris, A. Strasser, EMBO J. 19 (2000) 931–941.
[11] S. Balachandran, E. Thomas, G.N. Barber, Nature 432 (2004) 401–405.
[12] S. Balachandran, T. Venkataraman, P.B. Fisher, G.N. Barber, J. Immunol. 178 (2007) 2429–2439.
[13] J. Thorburn, F. Moore, A. Rao, W.W. Barclay, L.R. Thomas, K.W. Grant, S.D. Cramer, A. Thorburn, Mol. Biol. Cell 16 (2005) 1189–1199.
[14] K. Shimada, S. Matsuyoshi, M. Nakamura, E. Ishida, N. Konishi, J. Pathol. 206 (2005) 423–432.
[15] M.S. Jang, S.J. Lee, C.J. Kim, C.W. Lee, E. Kim, Oncogene 30 (2011) 471–481.
[16] M. Gomez-Angelats, J.A. Cidlowski, Cell Death Differ. 10 (2003) 791–797.
[17] E.C. Alappat, C. Feig, B. Boyerinas, J. Volkland, M. Samuels, A.E. Murmann, A. Thorburn, V.J. Kidd, C.A. Slaughter, S.L. Osborn, A. Winoto, W.J. Tang, M.E. Peter, Mol. Cell 19 (2005) 321–332.
[18] R.A. Screaton, S. Kiessling, O.J. Sansom, C.B. Millar, K. Maddison, A. Bird, A.R. Clarke, S.M. Frisch, Proc. Natl. Acad. Sci. U. S. A. 100 (2003) 5211–5216.

[19] C. Scaffidi, J. Volkland, I. Blomberg, I. Hoffmann, P.H. Krammer, M.E. Peter, J. Immunol. 164 (2000) 1236–1242.
[20] J.E. Allende, C.C. Allende, FASEB J. 9 (1995) 313–323.
[21] K. Ahmed, D.A. Gerber, C. Cochet, Trends Cell Biol. 12 (2002) 226–230.
[22] K. Niefind, B. Guerra, I. Ermakowa, O.G. Issinger, EMBO J. 20 (2001) 5320–5331.
[23] T. Buchou, C. Cochet, Med. Sci. (Paris) 19 (2003) 709–716.
[24] D.W. Litchfield, Biochem. J. 369 (2003) 1–15.
[25] F. Meggio, L.A. Pinna, FASEB J. 17 (2003) 349–368.
[26] O. Filhol, J.L. Martiel, C. Cochet, EMBO Rep. 5 (2004) 351–355.
[27] K. Izeradjene, L. Douglas, A. Delaney, J.A. Houghton, Oncogene 24 (2005) 2050–2058.
[28] M. Ruzzene, D. Penzo, L.A. Pinna, Biochem. J. 364 (2002) 41–47.
[29] C. Guo, S. Yu, A.T. Davis, H. Wang, J.E. Green, K. Ahmed, J. Biol. Chem. 276 (2001) 5992–5999.
[30] X. Xu, P.A. Toselli, L.D. Russell, D.C. Seldin, Nat. Genet. 23 (1999) 118–121.
[31] D. Llobet, N. Eritja, M. Encinas, N. Llecha, A. Yeramian, J. Pallares, A. Sorolla, F.J. Gonzalez-Tallada, X. Matias-Guiu, X. Dolcet, Oncogene 27 (2008) 2513–2524.
[32] S. Desagher, A. Osen-Sand, S. Montessuit, E. Magnenat, F. Vilbois, A. Hochmann, L. Journot, B. Antonsson, J.C. Martinou, Mol. Cell 8 (2001) 601–611.
[33] B. Guerra, O.G. Issinger, Curr. Med. Chem. 15 (2008) 1870–1886.
[34] M. Laramas, D. Pasquier, O. Filhol, F. Ringeisen, J.L. Descotes, C. Cochet, Eur. J. Cancer 43 (2007) 928–934.
[35] D.A. Gerber, S. Souquere-Besse, F. Puvion, M.F. Dubois, O. Bensaude, C. Cochet, J. Biol. Chem. 275 (2000) 23919–23926.
[36] V. Dupierris, C. Masselon, M. Court, S. Kieffer-Jaquinod, C. Bruley, Bioinformatics 25 (2009) 1980–1981.
[37] S. Sarno, H. Reddy, F. Meggio, M. Ruzzene, S.P. Davies, A. Donella-Deana, D. Shugar, L.A. Pinna, FEBS Lett. 496 (2001) 44–48.
[38] O. Filhol, A. Nueda, V. Martel, D. Gerber-Scokaert, M.J. Benitez, C. Souchier, Y. Saoudi, C. Cochet, Mol. Cell. Biol. 23 (2003) 975–987.
[39] O. Filhol, C. Cochet, Cell. Mol. Life Sci. 66 (2009) 1830–1839.
[40] A.A. Farooqui, J. Chromatogr. 184 (1980) 335–345.
[41] M.M. Savitski, S. Lemeer, M. Boesche, M. Lang, T. Mathieson, M. Bantscheff, B. Kuster, Mol. Cell. Proteomics 10 (2011) M110 003830.
[42] A. Deshiere, E. Duchemin-Pelletier, E. Spreux, D. Ciais, F. Combes, Y. Vandenbrouck, Y. Coute, I. Mikaelian, S. Giusiano, C. Charpin, C. Cochet, O. Filhol, Oncogene, 2013.
[43] L.A. Pinna, J. Cell Sci. 115 (2002) 3873–3878.
[44] A. Siddiqui-Jain, J. Bliesath, D. Macalino, M. Omori, N. Huser, N. Streiner, C.B. Ho, K. Anderes, C. Proffitt, Mol. Cancer Ther 11 (2012) 994–1005.
[45] M.A. McDonnell, D. Wang, S.M. Khan, M.G. Vander Heiden, A. Kelekar, Caspase-9 is activated in a cytochrome c-independent manner early during TNFalpha-induced apoptosis inmurine cells, Cell Death Differ. 10 (9) (2003) 1005–1015.
[46] L. Chantalat, D. Leroy, O. Filhol, A. Nueda, M.J. Benitez, E.M. Chambaz, C. Cochet, O. Dideberg, Crystal structure of the human protein kinase CK2 regulatory subunit reveals its zinc finger-mediated dimerization, EMBO J. 18 (11) (1999) 2930–2940.
[47] V. Moucadel, R. Prudent, C.F. Sautel, F. Teillet, C. Barette, L. Lafanechere, V. Receveur-Brechot, C. Cochet, Antitumoral activity of allosteric inhibitors of protein kinase CK2, Oncotarget. 2 (12) (2011) 997–1010.
[48] K. Bojanowski, O. Filhol, C. Cochet, E.M. Chambaz, A.K. Larsen, DNA topoisomerase II and casein kinase II associate in a molecular complex that is catalytically active, J Biol Chem. 268 (30) (1993) 22920–22926.